



Thermal conductivity of Al–Gd–TM glass-forming alloys

V. BYKOV, S. UPOROV, T. KULIKOVA

Institute of Metallurgy, Ural Branch, Russian Academy of Science, Amundsen str., 101, Ekaterinburg 620016, Russia

Received 17 July 2014; accepted 30 January 2015

Abstract: Thermal diffusivity, specific heat capacity and thermal conductivity of $\text{Al}_{86}\text{Gd}_6\text{TM}_8$ (TM = Cu, Ni, Co, Fe, Mn, Cr, Ti, Zr, Mo, Ta) glass-forming alloys in the temperature range of 300–880 K were determined by laser flash method. The temperatures of endothermic and exothermic reactions of the alloys were determined by differential scanning calorimetry method. The alloys were prepared by conventional arc-melting technique under helium atmosphere. All the alloys studied exhibit strong supercooling of the liquidus temperatures up to 80 K, which indicates their good glass-forming ability. The specific heat capacity of the alloys achieves the Dulong–Petit's value in the temperature range of 350–550 K except $\text{Al}_{86}\text{Cr}_8\text{Gd}_6$ and $\text{Al}_{86}\text{Zr}_8\text{Gd}_6$ compositions. The values of both thermal diffusivity and thermal conductivity of the alloy studied are significantly lower than those for pure aluminum. It is found that embedding 14% (mole fraction) of transition elements (Gd+TM) in the aluminum matrix leads to significant decrease in the absolute magnitudes of both thermal diffusivity and thermal conductivity in crystalline state. The thermal conductivity of glass-forming $\text{Al}_{86}\text{Gd}_6\text{TM}_8$ alloys is strongly affected by directed chemical bonding between alloy components.

Key words: Al-based alloys; thermal properties; specific heat capacity; thermal conductivity; thermal diffusivity

1 Introduction

In the last decades, Al-based alloys with additions of rare earth (RE) and transition metals (TM) have attracted increasing attention of researchers due to unique mechanical and corrosion properties [1–5]. These alloys have relatively high glass-forming ability that allows synthesizing them in form of amorphous ribbons by means of melt spinning technique. Furthermore, because of their unique physical properties in amorphous and crystalline states, these alloys have industrial applications such as corrosion resistant elements [3–5] and radio electronics components [6,7]. However, a number of important properties of these alloys such as thermal conductivity, thermal diffusivity and specific heat have not been sufficiently studied yet.

Earlier reports [8–12] indicated that the effective magnetic moments of rare earth elements in Al–RE and Al–TM–RE alloys are noticeably lower than those for trivalent RE ions. The similar results were obtained for Al–RE compounds by means of ab-initio calculation [13]. This abnormal behavior of magnetic properties was interpreted within the framework of conjecture about existence of covalent-like chemical bonding between

aluminum and RE which involves 4f-electron.

As reported in Refs. [14,15], the electronic and atomic structure of amorphous Al–Ni–La alloys indicates strong chemical interaction between aluminum and 3d-metal with a large portion of covalent type bonding. In particular, some researchers [14,15] claimed that a relatively high electrical resistivity (250–370 $\mu\Omega\cdot\text{cm}$) of amorphous alloys is caused by strong s–d hybridization. Non-magnetic behavior of 3d atoms in liquid aluminum alloys can also be explained by strong chemical bonding [16,17].

Recently, UPOROV et al [18] reported that the values of both electrical and the thermal conductivities of $\text{Al}_{83}\text{Co}_{10}\text{Ce}_7$ glass-forming alloy are relatively low in comparison with those for pure aluminum. Analyzing temperature dependence of Lorentz function, it can be found that the lattice contribution in total thermal conductivity is essential.

Therefore, it is obvious that the strong chemical bonding and associating should significantly affect the thermal conductivities of the alloys. The main goal of this study is checking the correlation between chemical bonding and thermal conductivity of the glass-forming $\text{Al}_{86}\text{Gd}_6\text{TM}_8$ alloys. For this purpose, thermal diffusivity, specific heat and thermal conductivity of alloys were

studied in the temperature range of 300–880 K.

2 Experimental

The samples of $\text{Al}_{86}\text{Gd}_6\text{TM}_8$ (TM = Cu, Ni, Co, Fe, Mn, Cr, Ti, Zr, Mo, Ta) alloys were prepared by conventional arc-melting technique using Centorr 5SA furnace under helium atmosphere. The initial components were aluminum (99.999%), gadolinium (99.86%) and corresponding transition metals with purity not less than 99.9%. All the specimens were re-melted five times to ensure homogeneity. The chemical composition of the alloys obtained was checked by atomic-emission method using the SpectroFlame Modula S analyzer.

The temperatures of endothermic and exothermic reactions of the alloys were determined by differential scanning calorimetry method using Netzsch STA 409 PC Luxx calorimeter. The thermal measurements were carried out during heating and subsequent cooling regimes at a rate of 10 K/min under argon flow (50 mL/min). The accuracy of determination of the temperature and enthalpy of reactions were ± 0.2 K and $\pm 5\%$, respectively.

Thermal diffusivity (a) of the alloys was determined by laser flash method (LFA) using Netzsch LFA 457 device in the temperature interval of 300–880 K under vacuum with the residual pressure of 0.1 mPa. The specimens for LFA investigations were prepared in form a rectangular parallelepiped with a square base of 10 mm and a thickness of 3–3.5 mm using IsoMet 5000 Buehler cut-off machine. The measurements were carried out in stepwise manner with the step of 50 K and the isothermal exposition of 20 min at each temperature. The specific heat capacity of the alloys at constant pressure (c_p) was calculated using standard comparison method [19]. Pure iron and Inconel 600 alloy were used as reference samples of specific heat. Previously, LFA device was calibrated with pure aluminum, iron and copper.

Densities (d) of the alloys at room temperature were determined by standard hydrostatic weighing method. The changes of densities of the alloys at temperature up to 880 K were taken into account using volume thermal expansion coefficient (β). The latter was obtained from the linear thermal expansion (α) data measured using the Netzsch 402CD dilatometer.

Thermal conductivity (λ) of the specimens was calculated using well-know relation $\lambda = adc_p$. The accuracy of determining the thermal diffusivity, specific heat and thermal conductivity of alloys were $\pm 1\%$, $\pm 3\%$ and $\pm 5\%$, respectively.

3 Results and discussion

The DSC data for $\text{Al}_{86}\text{Gd}_6\text{TM}_8$ alloys show series of

endo- and exo-thermal reactions at heating and cooling regimes. Analyzing DSC curves obtained under heating, solidus (T_s), liquidus (T_l) of alloys and supercooling (ΔT_l) of liquidus points (i.e., the difference between liquidus temperatures detected in heating and cooling modes) were identified. The obtained values of these thermal characteristics are listed in Table 1. It can be seen in Table 1 that no large distinctions in the solidus temperatures for all the alloys studied were found.

Table 1 Thermal characteristics of Al–Gd–TM alloys determined from DSC data

Composition of alloy	T_s/K	T_l/K	$\Delta T_l/\text{K}$
$\text{Al}_{86}\text{Cu}_8\text{Gd}_6$	892.6	1104.5	34.9
$\text{Al}_{86}\text{Ni}_8\text{Gd}_6$	905.2	1198.9	38.3
$\text{Al}_{86}\text{Co}_8\text{Gd}_6$	907.8	1252.7	21.9
$\text{Al}_{86}\text{Fe}_8\text{Gd}_6$	911.4	1290.4	32.2
$\text{Al}_{86}\text{Mn}_8\text{Gd}_6$	914.2	1266.4	23.4
$\text{Al}_{86}\text{Cr}_8\text{Gd}_6$	922.1	1296.2	26.6
$\text{Al}_{86}\text{Ti}_8\text{Gd}_6$	902.5	1257.7	81.0
$\text{Al}_{86}\text{Zr}_8\text{Gd}_6$	907.6	1169.4	26.1
$\text{Al}_{86}\text{Mo}_8\text{Gd}_6$	924.2	1323.8	45.3
$\text{Al}_{86}\text{Ta}_8\text{Gd}_6$	909.2	1320.9	30.9

In contrast, the differences between the liquidus points are significant for the alloys containing various types of transition metals. The noticeable supercooling observed for liquidus points is the typical phenomenon for Al-based glass-forming alloys [20,21] and also for good glass-forming system with strong interatomic interaction, such as SiO_2 . So, the existence of supercooling is one of the indirect evidences indicating strong chemical bonding between components of the alloys.

As was previously mentioned, the LFA device was calibrated with some pure metals, the comparison of results obtained for pure aluminum and iron metals with literature data is illustrated in Fig. 1. It is seen that our data are in satisfactory agreement with the results of other studies in whole temperature interval investigated.

Using comparison method [19], the study of specific heat capacity of $\text{Al}_{86}\text{Gd}_6\text{TM}_8$ alloys in the crystalline state up to 880 K was carried out. The experimental data obtained for the alloys were fitted by third order polynomial functions. The maximum deviations between fitted curves and experimental data do not exceed 2%. The results at different temperatures are shown in Table 2. It was established that the specific heat of the alloys took the Dulong–Petit's value ($3R=24.93$ J/(mol·K)) in the temperature range of 350–550 K for all samples except $\text{Al}_{86}\text{Cr}_8\text{Gd}_6$ and $\text{Al}_{86}\text{Zr}_8\text{Gd}_6$ compositions. The values of c_p for these

specimens are larger than 3R even at 300 K.

Using standard hydrostatic weighing method, we determined densities of the alloys at room temperature. Since densities of Al₈₆Gd₆TM₈ alloys are required for correct thermal conductivity calculation, additionally, we performed dilatometric measurements in the explored temperature range. It was found that the values of linear thermal expansion coefficients for the alloys studied are close to each other and significantly lower than those for pure aluminum metal. For example, at room temperature, linear thermal expansion coefficient of the Al₈₆Gd₆Ni₈ alloy $\alpha=(17\pm 1)\times 10^{-6} \text{ K}^{-1}$, whereas for pure aluminum $\alpha=(23\pm 1)\times 10^{-6} \text{ K}^{-1}$. Assuming that the linear thermal expansion of the samples is identical in all directions, we calculated volume thermal coefficient and densities of the Al–Gd–TM alloys using relations: $\beta=3\alpha$, $d=d_0(1-\beta T)$, where d_0 is the density of an alloy at 300 K.

Experimental thermal diffusivities obtained for the Al–Gd–TM alloys and corresponding thermal conductivities calculated are shown in Fig. 2. It can be seen that the dependencies of $a(T)$ and $\lambda(T)$ strongly demonstrate non-linear behavior. The absolute

magnitudes of both thermal diffusivity and conductivity are essentially lower than those for pure aluminum, especially for the Al₈₆Cr₈Gd₆ and Al₈₆Mo₈Gd₆ specimens. It should be noted that the Al₈₆Gd₆Cu₈ specimen has the largest a and λ among all the alloys investigated. It may be explained by low chemical activity of copper in the alloy because copper is actually noble metal. As reported in Ref. [25], relatively high thermal conductivity of binary Al–Cu alloys as well as weak monotonic concentration dependence of copper was observed. Thereby, it is supposed that copper in the Al–Gd–TM system also demonstrates metallic chemical bonding only. On the other hand, it is assumed that gadolinium and other TM metals contained in alloys investigated form covalent-like bonds. The strong chemical interaction between alloys components and hybridization of conductivity electrons cause essential changes in heat and charge transfer mechanisms. Thermophysical investigations performed for a number of Al-based alloys and other metallic systems with strong chemical bonding confirm this assumption. In particular, the similar behavior of thermal conductivity and high electrical

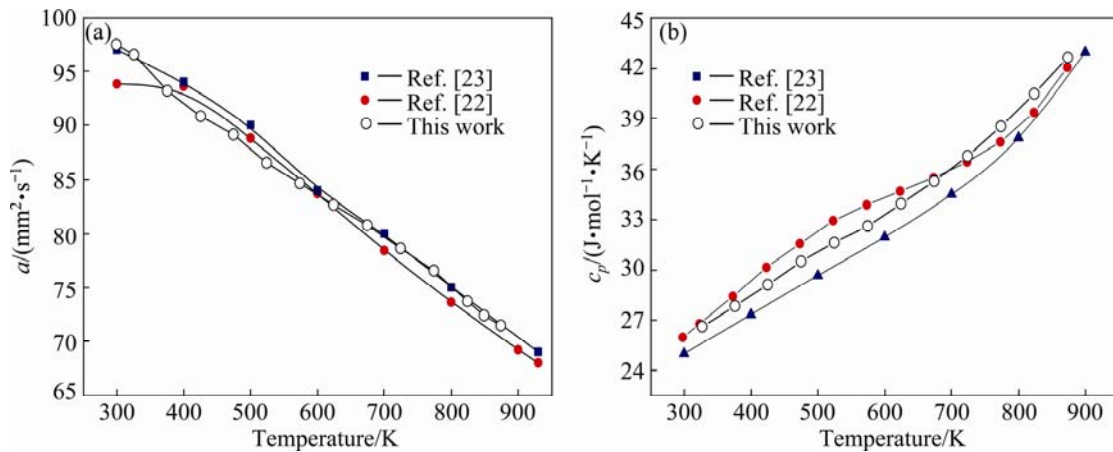


Fig. 1 Thermal diffusivity of aluminum (a) and heat capacity of iron (b)

Table 2 Specific heat capacity of Al–Gd–TM alloys at various temperatures

Composition of alloy	$c_p(\text{J}\cdot\text{mol}^{-1}\cdot\text{K}^{-1})$												
	320 K	370 K	420 K	470 K	520 K	570 K	620 K	670 K	720 K	770 K	820 K	880 K	
Al ₈₆ Cu ₈ Gd ₆	20.18	21.39	22.52	23.57	24.54	25.43	26.25	26.99	27.65	28.23	28.73	29.22	
Al ₈₆ Ni ₈ Gd ₆	23.31	24.37	25.33	26.20	26.97	27.65	28.24	28.73	29.13	29.43	29.64	29.77	
Al ₈₆ Co ₈ Gd ₆	23.69	25.00	26.06	26.90	27.54	28.03	28.39	28.66	28.88	29.07	29.27	29.58	
Al ₈₆ Fe ₈ Gd ₆	20.25	21.61	22.72	23.62	24.34	24.91	25.37	25.76	26.11	26.44	26.80	27.32	
Al ₈₆ Mn ₈ Gd ₆	23.10	24.21	25.22	26.13	26.94	27.66	28.27	28.79	29.20	29.53	29.76	29.90	
Al ₈₆ Cr ₈ Gd ₆	27.26	27.70	28.14	28.59	29.06	29.53	30.01	30.50	31.00	31.51	32.03	32.66	
Al ₈₆ Ti ₈ Gd ₆	22.58	23.69	24.73	25.68	26.56	27.35	28.07	28.70	29.25	29.73	30.12	30.49	
Al ₈₆ Zr ₈ Gd ₆	26.13	27.48	28.73	29.87	30.89	31.81	32.62	33.31	33.89	34.36	34.72	35.00	
Al ₈₆ Mo ₈ Gd ₆	24.50	26.27	27.77	29.01	30.01	30.77	31.32	31.67	31.82	31.80	31.62	31.20	
Al ₈₆ Ta ₈ Gd ₆	22.80	24.41	25.69	26.68	27.42	27.98	28.40	28.72	29.01	29.30	29.64	30.20	

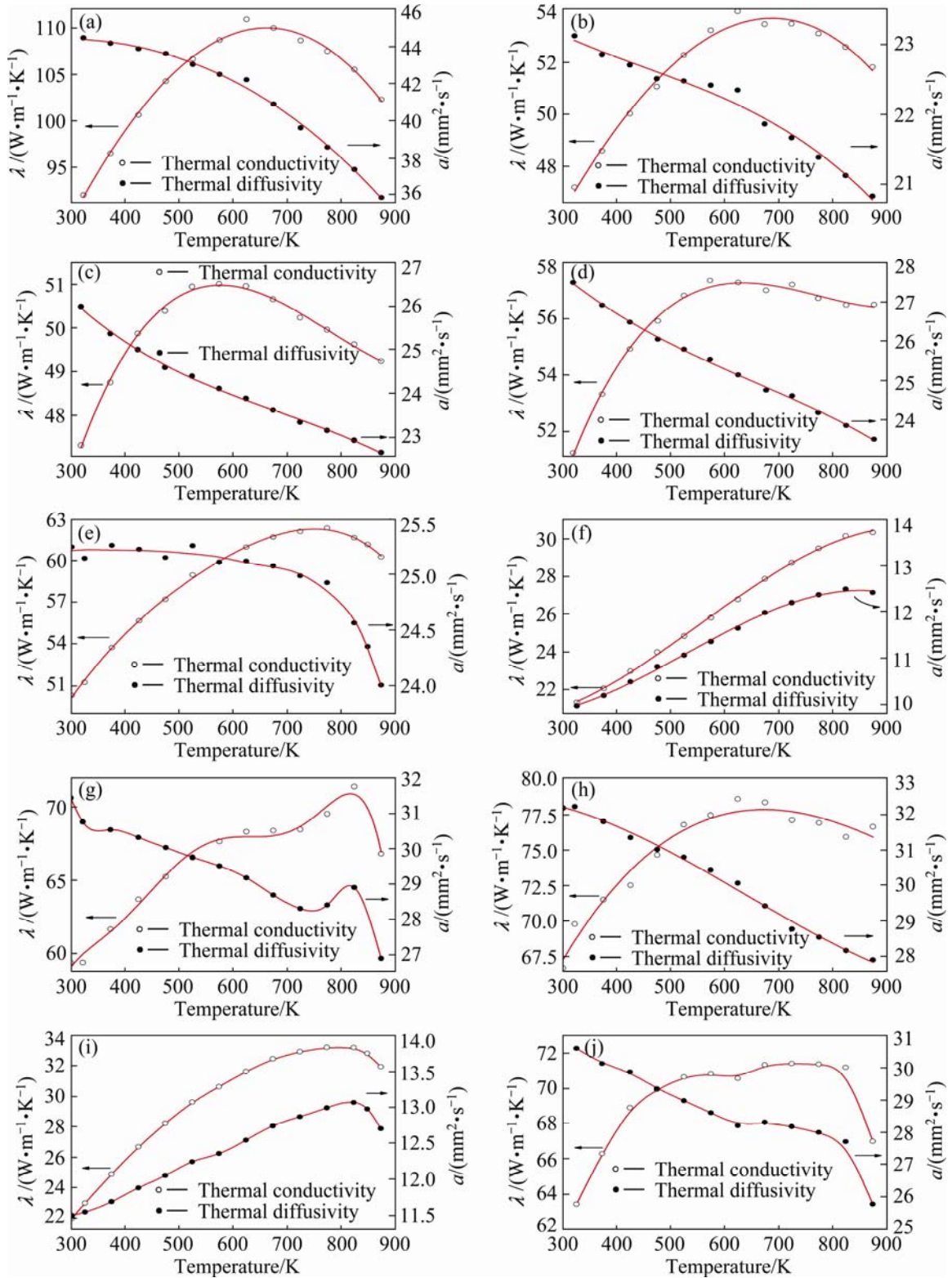


Fig. 2 Temperature dependency of thermal diffusivity and thermal conductivity of $Al_{86}Gd_6TM_8$ alloys: (a) Cu; (b) Ni; (c) Co; (d) Fe; (e) Mn; (f) Cr; (g) Ti; (h) Zr; (i) Mo; (j) Ta

resistivity were observed for the $Al_{83}Co_{10}Ce_7$ alloy [18]. The similar sharp decrease of thermal conductivity with increase of alloying elements concentration was found for Sc–Mg [26], binary magnesium and aluminum alloys [27–29]. The essential changes of thermal

conductivity may be caused by the decrease of valence electron concentration due to chemical interaction. The involvement of electrons into chemical bonding should affect thermal and electrical conductivities noticeably since both the heat and the charge transfers for metallic

system are basically caused by electrons. The experimental data obtained for the $\text{Al}_{86}\text{Gd}_6\text{TM}_8$ alloys confirm these assumptions.

4 Conclusions

1) All the alloys studied exhibit strong supercooling of the liquidus temperatures up to 80 K, which indicates their good glass-forming ability.

2) The specific heat capacity of the alloys achieves the Dulong–Petit's value ($24.93 \text{ J}/(\text{mol}\cdot\text{K})$) in temperature range of 350–550 K except $\text{Al}_{86}\text{Cr}_8\text{Gd}_6$ and $\text{Al}_{86}\text{Zr}_8\text{Gd}_6$ alloys. For the later, the specific heat capacity is larger than $3R$ even at room temperature.

3) 14% (mole fraction) of transition elements (Gd+TM) embedded in the aluminum matrix leads to a significant decrease in the absolute magnitudes of both the thermal diffusivity and the thermal conductivity in crystalline state.

4) The thermal conductivity of glass-forming $\text{Al}_{86}\text{Gd}_6\text{TM}_8$ alloys is strongly affected by covalent-like chemical bonding between alloy components.

Acknowledgements

The experimental results were obtained using the scientific instruments of the Collective Equipment Center “Ural-M”.

References

- INOUE A, OHTERA K, TSAI A P, MASUMOTO T. New amorphous alloys with good ductility in Al–Y–M and Al–La–M (M=Fe, Co, Ni or Cu) systems [J]. *Jpn J Appl Phys Lett*, 1988, 27: 280–282.
- INOUE A. Amorphous, nanoquasicrystalline and nanocrystalline alloys in Al-based systems [J]. *Prog Mater Sci*, 1998 43: 365–520.
- HOEKSTRA J G, QADRI S B, SCULLY J R, FITZ-GERALD J M. Laser surface modification of a crystalline Al–Co–Ce alloy for enhanced corrosion resistance [J]. *Adv Eng Mater*, 2005, 9: 805–809.
- SANSOUCY E, KIM G E, MORAN A L, JODOIN B. Mechanical characteristics of Al–Co–Ce coatings produced by the cold spray process [J]. *J Therm Spray Technol*, 2007, 16: 651–660.
- GOLDMAN M E, UNLU N, SHIFLET G J, SCULLY J R. Selected corrosion properties of novel amorphous Al–Co–Ce [J]. *Electrochem Solid-State Lett*, 2005, 8: 1–5.
- KUGIMIYA T, YONEDA Y. Single layer Al–Ni Interconnections for TFT-LCDs using direct contacts with ITO and a-Si [J]. *Kobelco Technol Rev*, 2007, 27: 8–12.
- LIU P, CHOU Y, HSU T, FUH C. Thin film transistor with Al–Ni–La alloy gate metallization technology [J]. *Electrochem Solid-State Lett*, 2011, 14: 57–59.
- SIDOROV V E, GORNOV O A, BYKOV V A, SON L D, SHEVCHENKO V G, KONONENKO V I, SHUNYAEV K Y. Magnetic studies of intermetallic compounds Al_3R (Al_{11}R_3) both in the solid and liquid states [J]. *J Non-Cryst Solids*, 2007, 353: 3094–3098.
- SIDOROV V, GORNOV O, BYKOV V, SON L, RYLITSEV R, UPOROV S, SHEVCHENKO V, KONONENKO V, SHUNYAEV K, ILYNYKH N, MOISEEV G, KULIKOVA T, SORDELET D. Physical properties of Al–R melts [J]. *Mater Sci Eng A*, 2007, 449–451: 586–589.
- BYKOV V A, SIDOROV V E, KULIKOVA T V, SHUNYAEV K Y. Magnetic susceptibility of dilute Al–Dy alloys at high temperatures [J]. *Bull Russ Acad Sci Phys*, 2008, 72: 1368–1370.
- UPOROV S, ZUBAVICHUS Y, YAROSLAVTSEV A, TROFIMOVA N, BYKOV V, RYLITSEV R, PRYANICHNIKOV S, SIDOROV V, SHUNYAEV K, MUDRY S, ZHOVNERUK S, MURZAKAEV A. Local chemical order in $\text{Al}_{92}\text{Ce}_8$ metallic glass: The role of 4f-electrons [J]. *J Non-Cryst Solids*, 2014, 402: 1–6.
- UPOROV S A, UPOROVA N S, SIDOROV V E, BELITYUKOV A L, LAD'YANOV V I, MEN'SHIKOVA S G. Magnetic susceptibility of the Al–Ni–REM and Al–Ni–Co–REM alloys [J]. *High Temp*, 2012, 50: 611–615.
- MAO Z, SEIDMAN D N, WOLVERTON C. First-principles phase stability, magnetic properties and solubility in aluminum–rare-earth (Al–RE) alloys and compounds [J]. *Acta Mater*, 2011, 59: 3659–3666.
- YAMAMOTO I, ZYTVELD J, ENDO H. Electronic and atomic structure of $\text{Al}_x\text{La}_{70-x}\text{Ni}_{30}$ amorphous alloys [J]. *J Non-Cryst Solids*, 1993, 156–158: 302–306.
- STADNIK Z M, MULLER F, STROINK G, ROSENBERG M. Magnetic behavior and hyperfine interactions in Al–Fe–Ce metallic glasses [J]. *J Non-Cryst Solids*, 1993, 156–158: 319–323.
- TERZIEFF P, AUCHET J. Electronic structure of 3d transition metal solutes in liquid aluminium [J]. *J Phys Condens Matter*, 1998, 10: 4139–4145.
- BRETONNET J L, AUCHET J. Electronic states of Fe, Co and Ni impurities in liquid aluminium [J]. *Phys Condens Matter*, 1991, 3: 7957–7961.
- UPOROV S A, BYKOV V A, YAGODIN D A. Thermophysical properties of the $\text{Al}_{83}\text{Co}_{10}\text{Ce}_7$ glass-forming alloy in crystalline and liquid states [J]. *J Alloys Compd*, 2014, 589: 420–424.
- SHINZATO K, BABA T A. Laser flash apparatus for thermal diffusivity and specific heat capacity measurements [J]. *J Therm Anal Calorim*, 2001, 64: 413–422.
- INOUE A, ONOUE K, HORIO Y, MASUMOTO T. Production of Al-based amorphous alloys by a metallic mold casting method and their thermal stability [J]. *Sci Rep Res Inst Tohoku Univ*, 1994, 39: 155–158.
- INOUE A. Stabilization of metallic supercooled liquid and bulk amorphous alloys [J]. *Acta Mater*, 2000, 48: 279–306.
- SHANKS H R, KLEIN A H, DANIELSON G C. Thermal properties of armco iron [J]. *J Appl Phys*, 1967, 38: 2885–2892.
- TOULOUKIAN Y S. Thermophysical properties of matter: The TPRC data series [M]. Vol 10. New York: IFI/Plenum, 1970.
- DESAI P D. Thermodynamic properties of iron and silicon [J]. *J Phys Chem Ref Data*, 1986, 15: 967–983.
- AKSÖZ S, OCAK Y, MARAŞLI N, ÇADIRLI E, KAYA H, BÖYÜK U. Dependency of the thermal and electrical conductivity on the temperature and composition of Cu in the Al based Al–Cu alloys [J]. *Exp Therm Fluid Sci*, 2010, 34: 1507–1516.
- RUDAJEVOVA A, BUCHB F, MORDIKEB B L. Thermal diffusivity and thermal conductivity of MgSc alloys [J]. *J Alloys Compd*, 1999, 292: 27–30.
- HO C Y, ACKERMAN M W, WU K Y, OH S G, HAVILL T N. Thermal conductivity of ten selected binary alloy systems [J]. *J Phys Chem Ref Data*, 1978, 7: 959–1177.
- PAN Hu-cheng, PAN Fu-sheng, YANG Ru-min, PENG Jian, ZHAO Chao-yong, SHE Jia, GAO Zheng-yuan, TANG Ai-tao. Thermal and electrical conductivity of binary magnesium alloys [J]. *J Mater Sci*, 2014, 49: 3107–3124.
- YU Kun, LI Shao-jun, CHEN Li-san, ZHAO Wei-shang, LI Peng-fei. Microstructure characterization and thermal properties of hypereutectic Si–Al alloy for electronic packaging applications [J]. *Transactions of Nonferrous Metals Society of China*, 2012, 22(6): 1412–1417.

Al–Gd–TM 非晶合金的导热性

V. BYKOV, S. UPOROV, T. KULIKOVA

Institute of Metallurgy, Ural Branch Russian Academy of Science,
Amundsena str., 101, Ekaterinburg 620016, Russia

摘要: 采用激光闪光法确定 $\text{Al}_{86}\text{Gd}_6\text{TM}_8$ (TM=Cu, Ni, Co, Fe, Mn, Cr, Ti, Zr, Mo, Ta) 非晶合金在 300~880 K 时的热扩散系数、比热容和导热系数。利用差示扫描量热法确定合金放热和吸热反应温度。在氦气保护下采用传统的电弧熔炼法制备合金。所有合金的液相线过冷度高达 80 K, 这表明它们具有很好的非晶形成能力。在温度为 350~550 K 时, 除 $\text{Al}_{86}\text{Cr}_8\text{Gd}_6$ 和 $\text{Al}_{86}\text{Zr}_8\text{Gd}_6$ 合金外, 其它合金的比热容都符合 Dulong–Petit 定则。合金的热扩散系数和导热系数值都远低于纯铝的。同时发现在铝基体中添加 14%(摩尔分数)的过渡元素(Gd+TM)会大大降低晶态合金热扩散系数和导热系数的绝对值。合金组份间化学键强烈影响非晶 $\text{Al}_{86}\text{Gd}_6\text{TM}_8$ 合金的导热系数。

关键词: 铝基合金; 热性能; 比热容; 导热系数; 热扩散

(Edited by Xiang-qun LI)